Bioactive Materials 20 (2023) 271–285

Contents lists available at ScienceDirect

Bioactive Materials

journal homepage: www.keaipublishing.com/en/journals/bioactive-materials

A novel gatifloxacin-loaded intraocular lens for prophylaxis of postoperative endophthalmitis

Mengna Li [a,b], Jing-Wei Xu [a,b], Jiayong Li [a,b], Wei Wang [a], Chenqi Luo [a,b], Haijie Han [a,b], Zhi-Kang Xu [c,**], Ke Yao [a,b,*]

[a] Eye Center, Second Affiliated Hospital, Zhejiang University School of Medicine, Hangzhou, 310009, PR China
[b] Zhejiang Provincial Key Laboratory of Ophthalmology, Hangzhou, 310009, PR China
[c] MOE Key Laboratory of Macromolecular Synthesis and Functionalization, Department of Polymer Science and Engineering, Zhejiang University, Hangzhou, 310027, PR China

ARTICLE INFO

Keywords:
Photocuring
Drug delivery intraocular lens
3D printing
Postoperative endophthalmitis
Gatifloxacin

ABSTRACT

Postoperative endophthalmitis (POE) has been the most threatening complication after cataract surgery, which perhaps can be solved by the antibiotic-loaded intraocular lens (IOL). However, most drug-loaded IOLs demonstrate insufficient drug quantity, short release time, increased implantation-related difficulties or other noticeable drawbacks. To prevent POE and to address these deficiencies, a drug-loaded copolymer IOL, prepared from poly (urethane acrylate) prepolymer, isobornyl methacrylate (IBOMA), N-vinyl-2-pyrrolidone (NVP), Irgacure 819, RUVA-93, and gatifloxacin (GAT), was rapidly fabricated via photocuring and by using a 3D-printed mold. This composite displayed an outstanding and controllable GAT release behavior *in vitro*, a high light transmittance, and a moderate refractive index. Also, it demonstrated improved strain stress and elongation compared with the reference commercial acrylic IOL material. *In vivo* tests demonstrated satisfying released drug concentration at the early treatment stage. *In vitro* and *in vivo* studies further confirmed the remarkable bacterial inhibition and prevention of POE by the proposed IOL, which also displayed good biocompatibility. These findings suggested that the GAT-loaded IOL could be a promising implant to prevent and cure POE, also the proposed methods could inspire more designs for various medical applications.

1. Introduction

Cataract, as the leading blind-causing eye disease, related to 51% of blindness worldwide with about 95 million individuals affected [1,2]. Cataract surgery with the intraocular lens (IOL) implantation has been the sole cure method so far. Though the surgery is a safe and highly developed approach, postoperative complications are presented. Among them, postoperative endophthalmitis (POE) has been the most dreaded complication, which leads to blindness and ocular atrophy. POE mostly occurs after cataract surgeries [3], with an incidence rate ranging from 0.012% to 1.3% [4–9] in the past two decades. Though topical antibiotics were routinely used preoperatively and one to two weeks postoperatively, it cannot efficiently prevent the occurrence of POE due to the poor bioavailability in deep ocular tissues. The European Society of Cataract & Refractive Surgeons recommended the intracameral injection of cefuroxime or moxifloxacin at the end of cataract surgeries to prevent POE [10]; however, this method prolongs the process, and there has been a risk of outflow of intracameral antibiotics and reflux of pathogens or contaminations in the anterior chamber in sutureless surgeries when an incision is incompletely closed. Hence, inserting an antibiotic-loaded drug delivery device, which releases continuously and works directly in target spot, would be a practical way to prevent POE.

The implantation of IOL has been a standard procedure in general cataract surgeries for decades. Thus, the necessity of using IOL in surgeries makes it a great drug delivery device which doesn't require extra surgical step. Previous studies focused on IOLs modification to prepare drug-loaded IOLs. Surface coating [11–17], chemical grafting [18–20], electrostatic interaction [21], and layer-by-layer self-assembly [22,23], which were all classified as surface modification techniques, have been studied. The ideas of creating extra drug-loading spaces on haptics were

Peer review under responsibility of KeAi Communications Co., Ltd.
* Corresponding author. Eye Center, Second Affiliated Hospital, Zhejiang University School of Medicine, Hangzhou, 310009, PR China.
** Corresponding author.
E-mail addresses: xuzk@zju.edu.cn (Z.-K. Xu), xlren@zju.edu.cn (K. Yao).

https://doi.org/10.1016/j.bioactmat.2022.05.032
Received 9 April 2022; Received in revised form 27 May 2022; Accepted 27 May 2022
2452-199X/© 2022 The Authors. Publishing services by Elsevier B.V. on behalf of KeAi Communications Co. Ltd. This is an open access article under the CC BY-NC-ND license (http://creativecommons.org/licenses/by-nc-nd/4.0/).

also reported [24,25]. Besides, drugs were deposited in an IOL polymer network by immersing the IOL into a drug solution [26,27] and by using the supercritical fluid impregnation method [28,29]. A number of patents were licensed on the field of drug-loaded IOLs; clinical trials about heparin-coated IOLs were performed [30–32] and heparin modified IOLs have already launched on the market. Nonetheless, no clinical trial concerning other kind of drug-loaded IOLs was performed or is currently running. All of the studies above have successfully modified an IOL into a sustained drug release device and some of them showed satisfying *in vivo* results; however, drawbacks such as insufficient drug quantity, short release time, increased difficulty of implantation, lack of *in vivo* studies, potential cytotoxicity or adverse reactions causes by the release of excess reagents and the need of terminal washing of the prepared system before use, have been noted in part of the studies. Therefore, the current study aims to develop an antibiotic-loaded IOL with a new practical method.

Besides the IOLs modification, an alternative way to create the drug-loaded IOLs is to blend the target drug with the monomer ingredient prior to polymerization rather than modifying the existing IOLs. With this method, those aforementioned imperfections could be improved; the device could be easy to implant, the quantity of the loaded drug and the drug release behavior could be manually controlled. To execute this method, the primary issue is how to maintain the drug stability. Previous studies have described the bulk photopolymerization of copolymers along with the target drugs and achieved controlled release of the entrapped drugs [33,34]. Though those researches were not relevant to ophthalmology or optical device, they provided the theoretical basis for our study. Photocuring, which is based on photopolymerization, offers an environmental-friendly process to rapidly convert liquid photosensitive oligomers and monomers into a solid substance at room temperature by the trigger of photoinitiators under UV or visible light exposure. Moreover, the monomers can be photocured in an enclosed mold to achieve a certain appearance. Though current technology of direct rapid prototyping of IOLs is not ready for primetime [35], rapid prototyping is still an efficient means to build a customized three-dimensional (3D) mold from liquid resin by using digital data. Digital light processing (DLP), as an additive manufacturing process in rapid prototyping technology [36], endows the printed product with precise details and exquisite surface finishes, its ability for shaping miniature model accurately makes it an ideal means to fabricate a transparent reverse mold of IOLs. The method combines photocuring and 3D-printed mold offers a fast polymerization process and a simple shaping method in a mild environment, this proposed approach not only avoids the high temperature and time-consuming thermopolymerization, but also eliminates the need for the laser shaping and aftertreatment processes that are involved in the traditional IOLs manufacture, thus it helps to retain the loaded quantity and keep the stability of the target drug to its largest extent.

Still, more issues, such as the optical properties and mechanical properties, must be considered in order to fabricate the qualified drug-loaded IOLs. Although acrylic IOLs get the biggest market share for its high transparency and good biocompatibility, unexpected issues such as haptic fracture [37] and optic disc breakage [38,39] have been reported, indicating the inadequate strength of the acrylate. Also, the presence of drug in a cross-linked network would reduce the mechanical strength of the polymer due to the plasticization effect. For this reason, a biofriendly substrate with outstanding mechanical properties is required. Polyurethane (PUR), a versatile material which could reach excellent mechanical properties, have been reported as a potential IOL material in studies, wherein PUR was described to have a high refractive index, excellent mechanical properties, a moderate cell adhesion properties, and it did not display cytotoxicity [40–43]. Moreover, when hydroxyl acrylates are used as blocking agent during PUR synthesis, the product, poly (urethane acrylate) (PUA), displays the advantages of both of its components, namely, the urethane bond and the acrylate functional group. Given its unique segmented block copolymeric character, PUA has been an emerging polymer material in the industry and has been meeting various expectations in terms of strength, toughness, flexibility, and transparency through switching ingredients during synthesis [44]. PUA can be obtained by photocuring from the nontoxic photosensitive PUA prepolymer; also, PUA prepolymer can copolymerize with other photosensitive monomers to achieve the desired properties of the final product. However, the use of PUA as a biomaterial in ophthalmology has not yet been reported and thus it is a promising area to research in optical biomaterial field.

The selection of antibiotics is also important for this study, since the target drug must be photostable and remain chemically inactive in the resin during the polymerization to keep the stability. Furthermore, it needs to be distributed well in the polymer in order to ensure the transparency of drug-loaded system. Gatifloxacin (GAT), a fourth-generation fluoroquinolone with good photostability, was chosen as the target drug in this study given its being a broad-spectrum antibiotic without a definite phototoxic effect [45]. It has showed efficient prevention and treatment on endophthalmitis [5,46,47] and its minimal inhibitory concentrations (MIC_{90}) against the most common cause of POE, *staphylococcus epidermidis (S. epidermidis)* [48], was 0.25–2 μg/mL [49,50]. GAT also shows great solubility and inert properties in some photosensitive chemicals, so it can be well distributed in the polymer matrix by adjusting the ingredients of the mixture for photocuring.

Herein, we describe a rapid fabrication method of a GAT-loaded IOL based on a bulk-synthesized PUA prepolymer, isobornyl methacrylate (IBOMA), N-vinyl-2-pyrrolidone (NVP), and adjuvants via photocuring in a 3D-printed mold. The major physical properties, the drug release profile along with the related factors, the biocompatibility, and the antibiotic effect of the newly designed device were evaluated in this study. To our knowledge, this proposed device is the first that involves the rapid casting of an IOL with sustained drug release ability, and it is also the first to combine a drug and resin before polymerization for preparing a drug-loaded IOL. This design could also be employed in loading other drugs to solve more ophthalmologic post-operative problems, and it could also inspire applications in fields other than the area of ophthalmologic biomaterial.

2. Materials and methods

2.1. Materials

Isophorone diisocyanate (IPDI), isobornyl methacrylate (IBOMA) and 2-(2′-hydroxy-5′-methacryloxyet hylphenyl)-2H-benzotriazole (RUVA-93) were purchased from J&K Chemical Ltd. (China). Dibutyltin dilaurate (DBTDL), N-vinyl-2-pyrrolidone (NVP) and hydroquinone were commercially obtained from Aladdin Industrial Corporation (China). Poly (tetramethylene ether) glycol 1000 (PTMG-1000), petroleum ether (30–60 °C), diethyl ether, phosphoric acid, triethylamine, acetonitrile were bought from Sinopharm Chemical Reagent Co. Ltd. (China). Hydroxypropyl acrylate (HPA) was purchased from Macklin Biochemical Co., Ltd. (China). Phenylbis (2,4,6-trimethylbenzoyl) phosphine oxide (Irgacure 819) was obtained from Sigma-Aldrich LLC. (USA). Phosphate-buffered saline solution (PBS 1 ×) and Trypsin-EDTA (with 0.25% trypsin and 0.02% EDTA) solution were bought from Genom Chemical Co., Ltd. (China). Dulbecco's modified Eagle's medium (DMEM/F12) was purchased from Corning Inc. (USA). Fetal Bovine Serum (FBS) was purchased from Biological Industries (Israel). Pentobarbital sodium was obtained from Merck&Co., Inc (Germany). Strain of *Staphylococcus epidermidis* ATCC 12228 was gained from Guangdong culture collection center (China). Human lens epithelial cells (hLECs) and adult retina pigment epithelium (ARPE-19) cells were provided by the Ophthalmology Lab Center, 2nd Affiliated Hospital of Zhejiang University School of Medicine. Hydrophobic acrylic FV-60A IOLs and its raw sliced material were purchased from 66 Vision Tech Co., Ltd. (China). GAT was generously offered by Shenyang Sinqi Pharmaceutical Co. Ltd. (China). Acetonitrile was of high performance liquid

chromatography (HPLC) grade and all other chemicals and solvents were analytical reagent and used without further treatment.

2.2. Generation of a digital model and 3D printing of a transparent mold

A two-piece mold was designed for the rapid preparation of IOL based on the prototype of a commercial enhanced C-loop IOL (FV-60A) at 1:1 ratio. The details of design were described in supplementary information (SI). The designs were digitally constructed using Rhinoceros (Version 5.0) and exported as an STL file for 3D printing. The transparent A370 photosensitive resin (Ausbond, China) was served as the 3D printing ink; designed structure was printed at a resolution of 25 μm using a Phoenix Touch Pro DLP 3D printer (Full Spectrum Laser, USA). The printed molds were repeatedly washed with ethanol and water to remove the uncured resin and were finely polished before use.

2.3. Preparation of GAT-loaded photopolymerizable IOL

2.3.1. Synthesis of PUA prepolymer

PUA prepolymer was synthesized via a two-step method (Fig. 1A) using a four-neck round-bottom flask in an oil bath under nitrogen environment. The flask was equipped with a mechanical stirrer, a condenser, a nitrogen port, and a thermometer. IPDI (8.8912 g, 0.04 mol) and the catalyst DBTDL (0.05% of total weight, 0.0173 g) were added, and the mixture was heated to 50 °C. Then PTMG-1000 (20.0000 g, 0.02 mol) was slowly dropped into the flask. The mixture was stirred

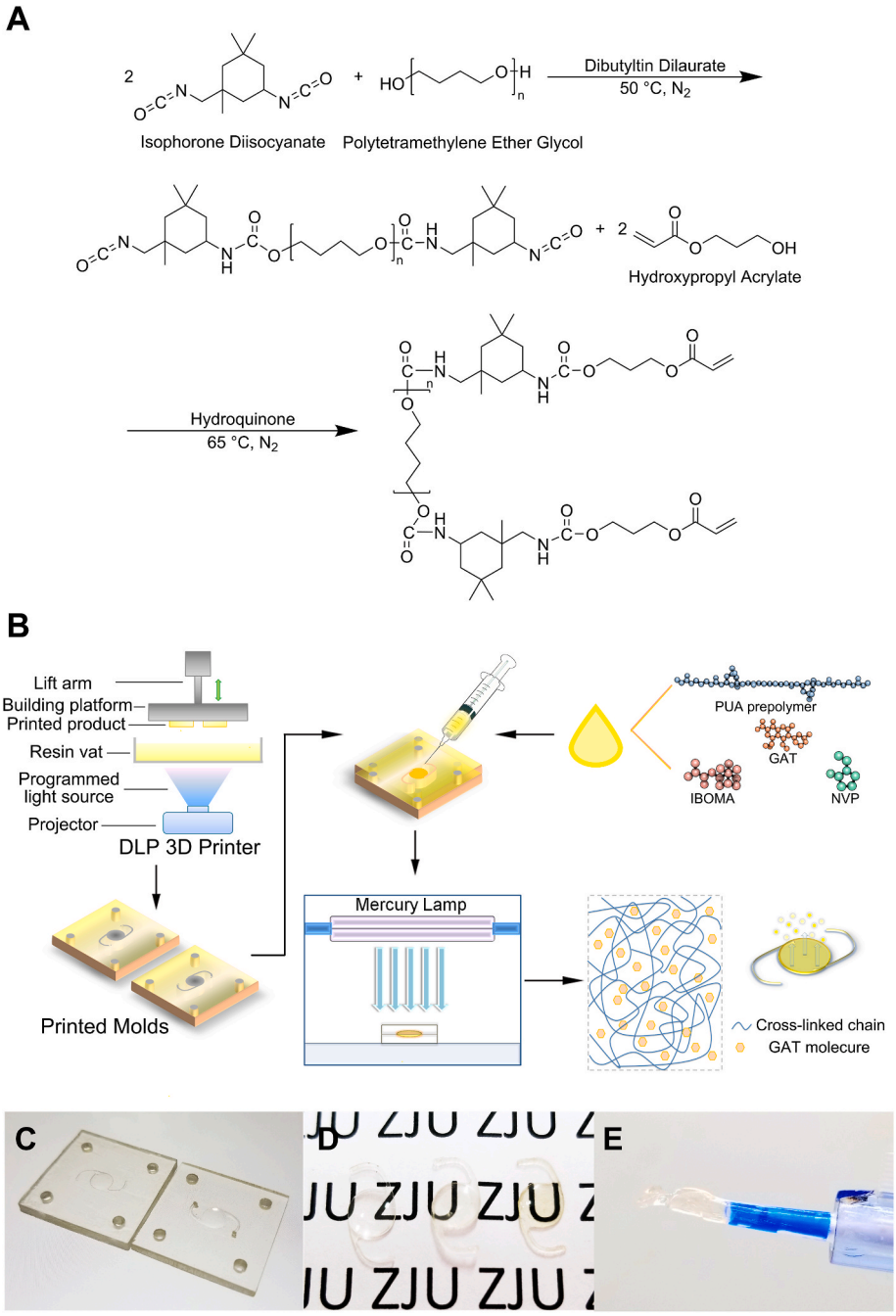

Fig. 1. Scheme of the synthesis of PUA prepolymer (A) and the rapid formation of PUA-GAT IOL by photopolymerization in the 3D printed molds (B); display of 3D printed molds (C) and 1:1 duplicated photocured IOLs (D): Prototype acrylic IOL (FV-60A), PUA-BLK IOL and PUA-GAT IOL (from left to right); (E) PUA-GAT IOL ejected from the IOL injection system.

for 3 h before adding hydroquinone (1% of HPA weight, 0.0574 g) as the inhibitor, and then HPA (5.7392 g, 0.042 mol) was introduced dropwise; the mixture was reacted continuously at 65 °C. The reaction was monitored by a TENSOR II FT-IR analyzer (Bruker, Germany) at certain time points; the reaction was stopped when the FT-IR spectrum indicated the disappearance of the absorption band from the –NCO group. The synthesized product was characterized by FT-IR and DD2-600 MHz 1H NMR (Agilent, USA), details concerning the spectra acquisition were described in SI.

2.3.2. Preparation of photopolymerizable composites and photocuring of the GAT-loaded/blank IOLs and sample strips

Two groups of materials, copolymer based on PUA with GAT (PUA-GAT) and without GAT (PUA-BLK), were prepared from a series of photosensitive resin mixtures by using PUA prepolymer as the main substance, IBOMA and NVP as the active diluents with different weight percentages, Irgacure 819 as the photoinitiator and RUVA-93 as the UV absorber with or without GAT. Each formulation was marked as B-a/b or G-a/b, where a/b represents the IBOMA/NVP mass ratio (Table 1). All mixtures were stirred thoroughly in brown bottles and allowed to stand at room temperature to remove any bubbles. The two pieces of 3D-printed molds were matched and fixed by bolts (Φ = 3.0 mm) threaded through the holes at each corner, with a polydimethylsiloxane films used as spacer (50-μm thick) inserted in between. The mixed resin was placed in a syringe and then injected into the molds through the vertical tunnel created on the molds. The molds were placed in a closed box, irradiated under a GGZ500 500W high-pressure mercury lamp (Yaming Lighting, China) at a distance of 20 cm, and cured for 5 min. Subsequently, the molds were opened and extra resin was injected to cover the shrunken surface. Next, the molds were fixed again, and the resin was cured for another 5 min (Fig. 1B). After demolding and trimming the edge of the photocured IOLs, the IOLs were washed in petroleum ether-diethyl ether solution (85:15, v/v) for three times (1 h) and then immersed in deionized water repeatedly to remove the uncured monomers. Finally, the products were dried overnight in a vacuum oven at room temperature. Meanwhile, cured sample strips for each group were prepared using the same procedure described above for material evaluation. The degree of crosslinking of samples was determined by solvent extraction method. All products were sealed separately, sterilized under ^{60}Co gamma-ray irradiation at 6 kGy (attained 10^{-6} Safety Assurance Level), and stored in the dark before use.

2.4. Material characterization

2.4.1. Basic characterization of PUA-BLK and PUA-GAT sample strips

The PUA-BLK and PUA-GAT samples were characterized by a Nicolet 6700 FT-IR Spectrometer (Thermo Scientific, USA), GAT was characterized by a TENSOR II FT-IR analyzer. X-ray diffraction (XRD) analysis was carried out by a X'Pert PRO diffractometer (PANalytical, Netherlands) to study the structural properties of PUA-BLK and PUA-GAT. The morphology of the cross-section of the whole series of sample strips was analyzed under a SU8010 scanning electron microscope (Hitachi, Japan). A direct observation of the presence and distribution of GAT in the PUA-GAT samples was done by IX71 inverted fluorescence microscopes (Olympus, Japan). The glass transition temperatures (T_g) of the PUA-GAT series were determined through dynamic mechanical analysis (DMA) by using a Q800 Dynamic Mechanical Analyzer (TA Instruments, USA). Details of those studies were described in SI.

2.4.2. Surface hydrophilicity test and swelling study

The sample strips of PUA-BLK and PUA-GAT were fixed on a glass slide for surface hydrophilicity determination. The water contact angle for the surface of the sample strips was measured by an OSA200 Optical Surface Analyzer (NBSI, China) and analyzed by Surface Meter Software (NBSI, China). Both contact angles of the sessile drop method on dehydrated samples and the captive bubble methods on fully hydrated samples were measured. Three random spots were tested for each sample, tests were performed in triplicate for each group, and the average value was calculated. Swelling studies were conducted on the series of PUA-BLK and PUA-GAT IOLs. The IOLs were weighted before soaking (W_d) and after soaking (W_m) in PBS for different time points at 37 °C, study was ended when the equilibrium state was reached. The maximum thickness and the diameter of optic part of the IOL were measured at dehydrated and fully hydrated status. Four samples were tested in each group and the average moisture content (MC) and dimensional change were calculated. MC was calculated using the following equation:

$$MC = \frac{W_m - W_d}{W_d} \times 100\%$$

2.5. In vitro drug release test

For the evaluation of the target drug release behavior *in vitro* under sink condition, the series of PUA-GAT IOLs were precisely weighed in dry condition before test, and four samples were prepared for each group. Samples were separately soaked in 1 mL PBS solution in 1.5 mL Eppendorf tubes, placed in a thermostatic oscillator set at 37 °C, 100 rpm. Then each sample was picked out from the current tube and transferred into a new Eppendorf tube filled with 1 mL fresh PBS medium at fixed time points; the new tubes were placed back to the oscillator and the used tubes containing the 1 mL GAT-released medium were collected. The concentration of GAT in each release medium was determined based on UV absorbance at 290 nm by using a Nanodrop 2000c (Thermo Scientific, USA), and the cumulative release of GAT in each group was calculated. The released medium also was tested by a LC20 HPLC (Shimadzu, Japan) and a 6460 Series Triple Quadrupole LC/MS system (Agilent, USA) to study the chemical stability of GAT, meanwhile, the quantity of eluted GAT during the washing process in Section 2.3.2 was measured; details of those studies were described in SI.

Table 1
Formulas of blank/GAT loaded photosensitive copolymer.

	Name	PUA prepolymer (weight ratio)	IBOMA	NVP	RUVA-93	Irgacure 819	GAT
PUA-BLK	B-0/40	60	0	40	1	0.1	0
	B-5/35	60	5	35	1	0.1	0
	B-10/30	60	10	30	1	0.1	0
	B-15/25	60	15	25	1	0.1	0
	B-20/20	60	20	20	1	0.1	0
PUA-GAT	G-0/40	60	0	40	1	0.1	1
	G-5/35	60	5	35	1	0.1	1
	G-10/30	60	10	30	1	0.1	1
	G-15/25	60	15	25	1	0.1	1
	G-20/20	60	20	20	1	0.1	1

2.6. Optical performance evaluation

The sample strips of the PUA-BLK and PUA-GAT were fully hydrated in PBS and placed perpendicular to the light beam in the PBS-filled cuvette. Light transmittance was analyzed at 200–800 nm by a UV-2450 UV–Vis Spectrophotometer (Shimadzu, Japan). Light transmittance of PUA-GAT was also tested at the beginning of drug release in PBS and after 4 weeks of GAT release. The refractive index of the hydrated samples at the wavelength of 589 nm were measured in air by a M2000 Ellipsometer (J.A. Woollam, USA). The incidence angle was set at 60° and the glass with transparent film model was employed to obtain the refractive index. The tests were performed in triplicate with three spots per sample at 20 °C, and the average was calculated.

2.7. Mechanical properties evaluation

The cured sample strips of PUA-BLK, PUA-GAT, and the reference FV-60A material were cut into type 1BB dumbbell-shaped test specimens as described in ISO 527–2 [51] for tensile stress–strain analysis. The stress–strain analysis was performed by a CMT6103 Electronic Universal Testing Machine with a 0–1 k*N* capacity (Xinsansi, China) at a strain rate of 5 mm/min at room temperature. Sand papers were applied in the clamps to ensure the good grip of samples. Dry samples of PUA-BLK and PUA-GAT were measured for their ultimate tensile strength and elongation at break performance. For the evaluation of the mechanical properties of PUA-GAT materials at working condition, samples from this group and FV-60A group were soaked in PBS solutions for fixed times before measurement and then the dynamic change in the above-mentioned mechanical indicators were observed. Tests were performed in quintuplicate for each group, and the average values were adopted.

Finally, the optimum formulation for PUA-GAT IOL was selected according to the result of the comprehensive assessment of drug release behavior, optical performance, and mechanical properties for later studies.

2.8. In vitro cytotoxicity test

A cytotoxicity elution test involving APRE-19 and hLECs cells was performed *in vitro* to assess the cytotoxicity of the PUA-BLK and PUA-GAT IOLs. Cell viability was tested by Cell Counting Kit-8 (CCK-8) assay (Dojindo, Japan) after culture according to the manufacturer's protocol. The mechanism of CCK-8, preparation of elution media and details of culture [52] were described in SI. Optical density values at 450 nm were measured by an iMark microplate absorbance reader (Bio-rad, USA), and the cell viability was calculated.

2.9. In vitro antibacterial test

To evaluate if the PUA-GAT IOL could inhibit and eliminate the pathogen fast, the *S. epidermidis* ATCC 12228 strain, a standard strain for antibacterial activity tests, was selected as the model bacteria to examine the antibacterial activity of PUA-GAT IOL. The details of bacterial culture were described in SI. Diluted bacterial suspension (1 mL) consisting of 1×10^6 CFU/mL was added into each well of a 24-well plate; for the three experimental groups, a piece of PUA-GAT IOL, PUA-BLK IOL or FV-60A IOL was immersed in the bacterial suspension-contained well respectively (n = 3). Meanwhile, 2 μL GAT solution (1 mg/mL) was added into the wells of the positive control group, and nothing was added in the wells of the negative control group. The plate was incubated at 37 °C for 24 h; the bacterial suspension of each well was collected. Suspensions were subjected to fluorescent dyeing by using an L-7012 LIVE/DEAD BacLight Bacterial Viability Kit (Invitrogen, USA) according to the manufacturer's protocol. The viability of *S. epidermidis* was observed and captured under an IX71 inverted fluorescence microscope (Olympus, Japan), the details of filter setting were described in SI.

2.10. In vivo study

2.10.1. Animals and care

All animal procedures were performed according to the approved Zhejiang University Institutional Animal Care and Use Committee protocol and in accordance with the requirements of the Association for Assessment and Accreditation of Laboratory Animal Care International.

White New Zealand rabbits of either gender, weighing 2.1 ± 0.3 kg, were purchased from an approved breeding facility in Hangzhou, China. Each rabbit was housed in an individual cage, reared at room temperature (24 ± 2 °C) and at 12 h/12 h light–dark cycle, and was given free access to water and feeds. The eyes of all the rabbits to be subjected to operation were treated with topical levofloxacin and 1% atropine eye gel preoperatively. The rabbits underwent general anesthesia with 3% pentobarbital sodium and local anesthesia with 0.5% proparacaine hydrochloride ophthalmic solution before surgery. All operated eyes were treated with topical prednisolone acetate and 1% atropine eye gel for 2 weeks, in addition to the topical diclofenac sodium for 4 weeks postoperatively.

2.10.2. Biocompatibility study design

Nine rabbits were divided into three groups, wherein all rabbits underwent a standard phacoemulsification with IOL implantation in one eye after skin preparation and draping, as follows:

Group I: Phacoemulsification and implantation of FV-60A IOL;
Group II: Phacoemulsification and implantation of PUA-BLK IOL;
Group III: Phacoemulsification and implantation of PUA-GAT IOL.

IOLs were implanted at dehydrated status with the Viscoject eco IOL injection systems (Medicel A.G., Switzerland). Postoperative follow up, as described in Section 2.10.5, was conducted at a fixed time to evaluate the biocompatibility of the novel IOLs *in vivo*.

2.10.3. In vivo drug release study

All the operated eyes mentioned in Section 2.10.2 underwent anterior chamber paracentesis at fixed time points postoperatively under general and local anesthesia, approximately 100–150 μL of aqueous humor was carefully extracted for drug quantification. All the operated eyes of group I were dosed with GAT eye gel 1 h before the aqueous humor sample collection, and samples from group II were used as blank control. All collected samples were stored at −80 °C until analysis. GAT concentration in aqueous humor was determined by HPLC, the optimum condition was described in SI.

2.10.4. Antibacterial activity study design

For further assessment of the efficacy of the drug-loaded IOL in preventing bacterial intraocular endophthalmitis, an animal model was established by using *S. epidermidis* as the model bacteria. Bacterial suspension (30 μL) at 10^7 CFU/mL was inoculated into the anterior chamber of the operated eye one day after surgery, whereas an equal volume of normal saline (NS) was injected to the control group. Each group owns six rabbits, the rabbits were randomly grouped as follows:

Group A: Phacoemulsification and implantation of FV-60A IOL, NS-inoculated;
Group B: Phacoemulsification and implantation of FV-60A IOL, *S. epidermidis*-inoculated;
Group C: Phacoemulsification and implantation of PUA-GAT IOL, *S. epidermidis*-inoculated.

2.10.5. Follow-ups

All operated eyes described in Sections 2.10.2 and 2.10.4 were examined under a YZ5S slit lamp microscope (66 Vision, China) before surgery and at fixed time points after operation until sacrifice. Ocular inflammatory and infectious symptoms, including ciliary injection,

exudation, synechia, hyphema, and hypopyon, were noted; also, conjunctival injection [53], chemosis [53], corneal opacity [54], aqueous flare [55] and cells [55] were graded and scored via a blind method involving the use of referenced classification criteria (SI in Tables S1–5). Corneal endothelial cell density was measured pre-operatively and on day 29 post-operation by using an EM-3000 specular microscope (Tomey, Japan). In addition, the intraocular pressure (IOP) of all the operated eyes were measured by an NT-510 non-contact tonometer (Nidek, Japan) pre-operatively and on day 29 post-operation; the IOP of each eye was measured three times, and the average was calculated.

2.10.6. Aqueous humor culture and bacteria identification

When hypopyon or aqueous exudation was found during the post-operation examinations, aqueous humor samples were collected for subsequent bacterial culture and identification. In brief, 100 μL of the collected sample from each eye was separately dropped onto tryptic soy agar plates, which were cultured at 37 °C for 24 h. The bacterial colonies that grew on the plates were obtained and identified by a MALDI Biotyper (Bruker Daltonik, Germany) for matching with a bacterial reference database.

2.10.7. Pathological morphology and histological examination

All rabbits were sacrificed on day 29 post-operation. Pathological examinations were performed following ocular enucleation. The ocular dimensions were measured and compared with those of the contralateral eye. Fixation, dehydration, embedding, slicing, and hematoxylin–eosin staining were performed using the standard procedure. The prepared tissue sections were observed under a biological microscope to examine the cornea, anterior chamber, iris, and retina of each group.

2.11. Statistical analysis

Data are presented as mean ± SD. All statistical analyses were carried out using GraphPad Prism v9.3 (GraphPad Software, USA), and two-way analysis of variance (two-way ANOVA) or multiple t tests was used according to the circumstance. Statistical significance was set at $P < 0.05$.

3. Results

3.1. Prepolymer characterization, 3D-printed mold creation, and IOL photocuring

A transparent and viscous PUA prepolymer was synthesized according to the reaction scheme. Both FT-IR and 1H NMR spectra in Figs. S1 and S2 of SI showed that the synthetic prepolymer displayed the expected chemical structures. A digital structure for 3D printing was generated (SI in Fig. S3), and Fig. 1C showed the obtained product of the 3D-printed molds, wherein the product displayed a fine detail and a smooth surface. The shape of the cured materials in the mold was perfectly duplicated at 1:1 ratio from the prototype IOL, PUA-BLK IOL

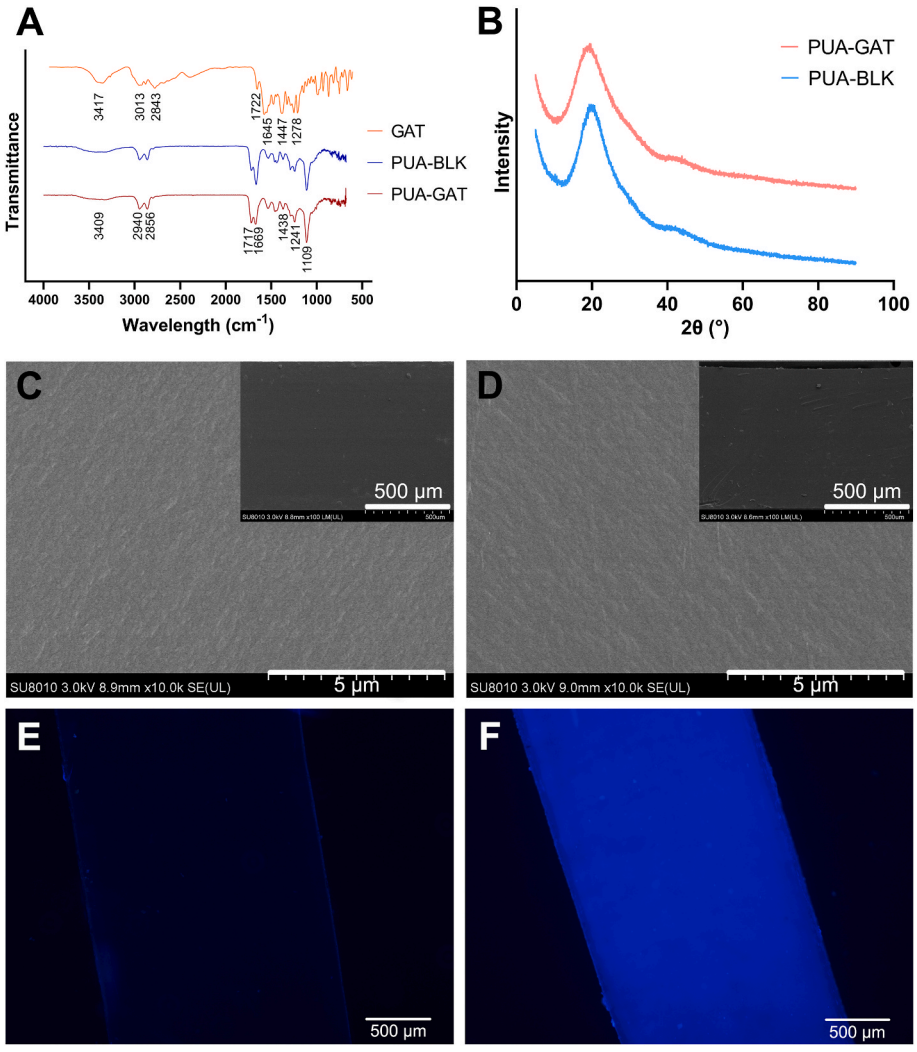

Fig. 2. The FT-IR spectra of GAT, B-5/35 of PUA-BLK and G-5/35 of PUA-GAT (A); the XRD analysis of B-10/30 of PUA-BLK and G-10/30 of PUA-GAT (B); the SEM image of B-10/30 of PUA-BLK (C) and G-10/30 of PUA-GAT (D) demonstrated similar even and compact texture structure of the cross-section, no change of microscale structure caused by the GAT was observed; the fluorescent determination of B-10/30 of PUA-BLK (E) and G-10/30 of PUA-GAT (F) showed positive fluorescent effect (blue luminescence) on PUA-GAT and vague fluorescent effect on PUA-BLK.

was colorless, whereas PUA-GAT IOL displayed a yellow-tinted transparent appearance (Fig. 1D). Moreover, PUA-GAT IOL was foldable, and it fitted the commercial IOL injection system (Fig. 1E). The degree of crosslinking was gradually increased with increasing IBOMA/NVP ratio (SI in Table S6).

3.2. Material characterization

FT-IR spectra of the GAT, PUA-BLK and PUA-GAT samples were shown in Fig. 2A (also in SI Fig. S4). The characteristic bands of GAT were assigned as following groups: 3417 cm^{-1} (O–H), 3013, 2843 cm^{-1} (C–H), 1722 cm^{-1} (C═O, from carboxylate), 1645 cm^{-1} (C═O, from pyridone), 1447 cm^{-1} (C–C, C–N) and 1278 cm^{-1} (C–F, C–O). The spectra of PUA-BLK and PUA-GAT showed the following peaks: 3409 cm^{-1} (O–H), 2940, 2856 cm^{-1} (C–H), 1717, 1669 cm^{-1} (C═O), 1438 cm^{-1} (C–C, C–N), 1241 cm^{-1} (C–O, C–F) and 1109 cm^{-1} (C–O). Compare to the PUA-BLK spectrum, a stronger absorption of PUA-GAT at 1717 cm-1 was seen, which can be explained by the presence of GAT in the PUA-GAT samples.

The XRD spectra of PUA-BLK and PUA-GAT were shown in Fig. 2B, wherein the characteristic peaks of PUA-BLK and PUA-GAT were observed at 19.78° and 18.96° respectively. The peak of PUA-GAT was shifted to a lower diffraction angle, which indicated the entrapment of GAT in the samples.

The cross-section structure of PUA-BLK and PUA-GAT samples as seen under SEM was shown in Fig. 2C and D. The similar even and compact texture was observed in both groups, suggesting that the incorporated GAT in the crosslinked polymer network did not cause any noticeable change in the microstructure. In addition, no obvious microstructure change was found in PUA-GAT after 4 weeks of drug eluting (SI in Fig. S5).

The fluorescence of the tested samples from the PUA-BLK and PUA-GAT groups was compared under microscope. Clearly, a vague fluorescence came out from the PUA-BLK samples (Fig. 2E), whereas an obvious fluorescence observed as blue luminescence due to the fluorescent properties of GAT, was presented uniformly in all fields of the PUA-GAT samples (Fig. 2F), which demonstrated the presence of GAT and its uniform distribution in the network.

The T_g of the PUA-GAT materials was shown in Table 2. The T_g values gradually increased with increasing IBOMA/NVP ratio. The temperatures at the onset of E' were all below −20 °C, which was beyond the range; the T_g values as determined by the peak of E'' were all within the room temperature range. G-0/40 was not completely subjected to the test as it was yielded during the heating process, making the obtained result invalid.

3.3. Surface hydrophilicity and swelling capacity

Hydrophilic contact angles of the PUA-BLK and PUA-GAT samples under the two different measure methods were presented in Fig. 3A and B. With the increasing IBOMA/NVP mass ratio, the contact angle of PUA-GAT and PUA-BLK increased in sessile drop method and decreased in captive bubble method, indicating that the material surface was becoming less hydrophilic. Still, they were less hydrophobic than the referenced hydrophobic material FV-60A. As shown in Fig. 3C, the final MC of PUA-BLK and PUA-GAT samples were all less than 10%, and they were decreased when the IBOMA/NVP mass ratio increased. The comparing of MC between PUA-BLK and PUA-GAT groups under the same IBOMA/NVP ratio showed no significant differences ($P > 0.05$). The hydration process was presented in Figure S6 of SI. Dimensional change of IOLs was not obvious in all groups (SI in Table S7).

Table 2
Data on the glass transition temperature (T_g) of PUA-GAT samples.

Group	T_g by E'' (°C)	T_g by Tanδ (°C)
G-0/40	n.d.	n.d.
G-3/35	19.3	51.5
G-10/30	20.1	57.4
G-15/25	25.9	57.9
G-20/20	26.4	68.7

n.d. – not determined. Tanδ – mechanical loss coefficient, tan$\delta = E''/E'$.

3.4. In vitro drug release study

The chemical stability of eluted GAT from our material was confirmed by HPLC and MS (SI in Fig. S7), and about 4.75–8.53% of GAT was lost during the monomer laundry steps (SI in Table S8). As shown in Fig. 3D, GAT release was sustained for up to at least 40 days in all groups. A decreasing IBOMA/NVP mass ratio expedited the release speed and increased the cumulative release of GAT; also, it promoted the burst release at the early stage. On the long-term basis (16 days–40 days), the release rate was highest in G-10/30. Finally, 5.10 ± 0.14 μg/mg of GAT of G-10/30 samples was released during the 40 days.

3.5. Optical properties

As shown in the UV–vis spectra (SI in Fig. S8), the light transmittance of the sample strips from all groups was sufficiently high at 94%–98% in the visible spectrum. The light transmittance of G-10/30 sample from wavelengths of 500 nm–800 nm was almost the same as that of B-10/30 sample (Fig. 4A), indicating the effect of GAT on light transmittance is negligible. The UV-C and UV-B light were all blocked from wavelengths of 200 nm–320 nm and UV-A light was partially screened from 320 nm to 380 nm. PUA-GAT samples remained high light transmittance after 28 days of GAT release (Fig. 4B), suggesting the drug release process was not closely related to the material transparence. Table 3 showed the refractive index of the tested groups; no significant difference was found among the tested groups ($P > 0.05$).

3.6. Mechanical properties

The ultimate tensile strength and the elongation at break of the test materials varied with the change in IBOMA/NVP mass ratio and with the presence of GAT. As the ratio increased from 0/40 to 20/20, the ultimate tensile strength of both the PUA-BLK and PUA-GAT samples increased gradually from 15.4 to 14.4 Mpa to 35.3 and 33.3 Mpa, respectively (Fig. 5A). However, the elongation was nonlinearly dependent on IBOMA/NVP ratio; the maximum value was obtained at the B/G-10/30 groups, whereas the minimum was obtained at the B/G-5/35 groups. In particular, the values for elongation of PUA-BLK and PUA-GAT were 153%–203% and 193%–228%, respectively (Fig. 5B). As for the comparison of the elongation of PUA-BLK and PUA-GAT consisting of the same IBOMA/NVP ratio to determine the mechanical effect of GAT, the performance of PUA-GAT was always higher than that of PUA-BLK ($P < 0.05$).

The dynamic change in ultimate tensile strength and elongation of the PUA-GAT samples in solution for up to 8 weeks was presented in Fig. 5C and D; soaking time and IBOMA/NVP ratio have effectively influenced the mechanical properties of the PUA-GAT samples. A marked decline in ultimate tensile strength of each tested group after soaking was observed in the first 2 weeks and then began to level off; no significant change was observed at weeks 2, 4, and 8 ($P > 0.05$). Compared with the ultimate tensile strength of the hydrophobic acrylate sample at the same time point, that of all the tested PUA-GAT samples was significantly higher ($P < 0.05$), except for the G-5/35 group at weeks 4 and 8. As for the elongation, the results for all samples from G-10/30, G-15/25, and G-20/20 at each time point after being soaked ranged from 184% to 216%, which were significantly higher than that of the reference FV-60A measured as 98% ($P < 0.05$). The G-0/40 samples were too weak to be subjected to the test after being soaked; thus, their results were excluded.

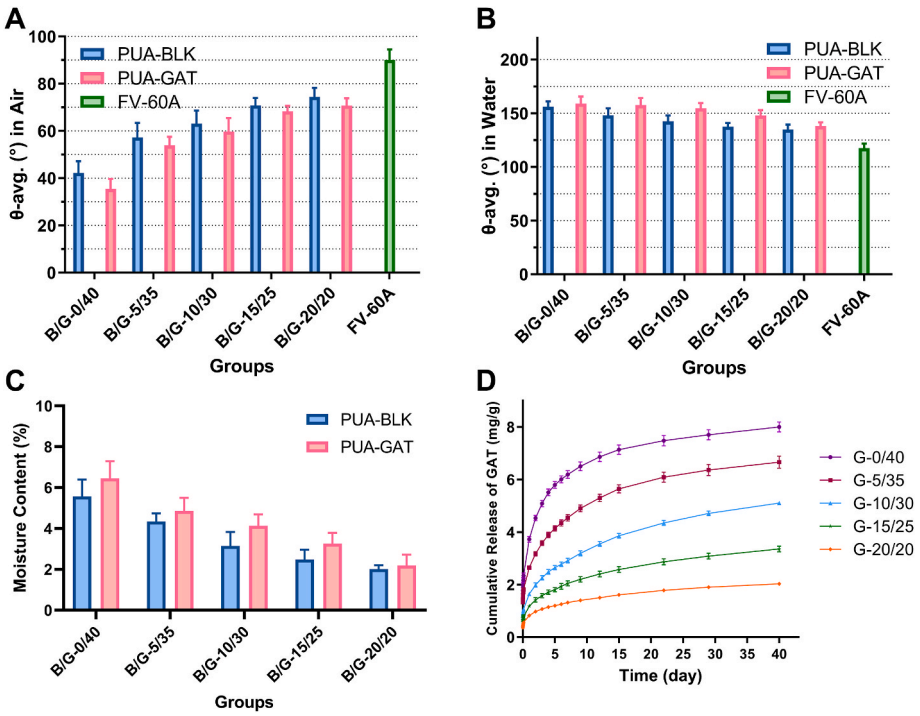

Fig. 3. Contact angle of PUA-BLK and PUA-GAT with sessile drop method (A) and captive bubble method (B); (C) the moisture content of PUA-BLK and PUA-GAT ($P > 0.05$, multiple t tests); (D) in-vitro release profiles of GAT from PUA-GAT IOL with different IBOMA/NVP mass ratio, wherein the mg/g indicated the mass of released GAT in relation to the mass of the dehydrated IOL.

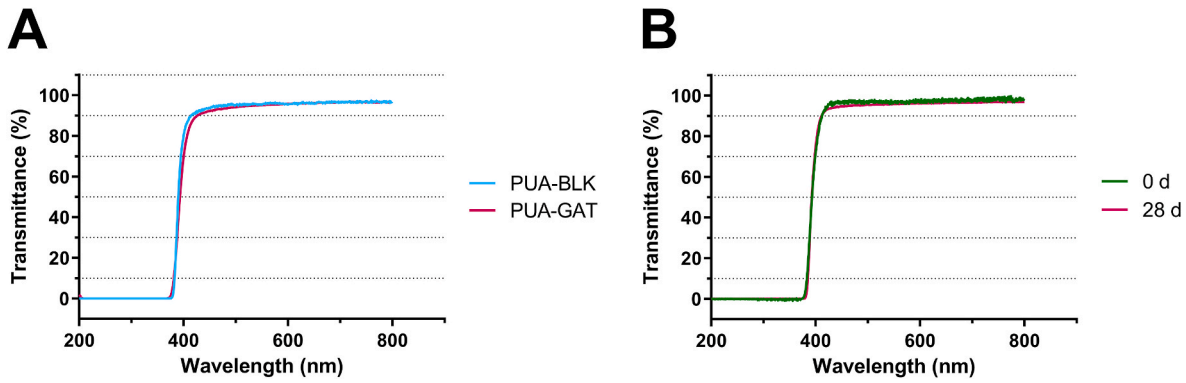

Fig. 4. UV–vis spectra of the 1 mm thick B-10/30 of PUA-BLK and G-10/30 of PUA-GAT samples immersed in PBS (A); UV–vis spectra of G-10/30 of PUA-GAT samples at the beginning and after 28 days of GAT release (B).

Table 3
Refractive index of PUA-BLK and PUA-GAT samples.

Group	B/G-0/40	B/G-5/35	B/G-10/30	B/G-15/25	B/G-20/20
PUA-BLK	1.490 ± 0.007	1.492 ± 0.010	1.496 ± 0.007	1.493 ± 0.008	1.495 ± 0.008
PUA-GAT	1.491 ± 0.003	1.491 ± 0.006	1.491 ± 0.006	1.496 ± 0.010	1.499 ± 0.005

$P > 0.05$, two-way ANOVA.

On this basis, combined with the results of the tests for release behavior and optical performance, G-10/30 was selected as the optimum formulation. The novel IOLs produced using this formulation were used for later evaluations.

3.7. *In vitro cytotoxicity study*

The cytotoxicity of the extracting solution from PUA-BLK and PUA-GAT IOLs toward ARPE-19 and hLECs were evaluated by CCK-8, and the percent cell viability in relation to the negative control (NC) was shown in Fig. 6A and B. The result suggested that there was no significant difference in cell viability among the PUA-BLK IOL, PUA-GAT IOL, FV-40A IOL or NC group at 24, 48, and 72 h ($P > 0.05$), and the cell viability of the abovementioned groups are much higher than that of the cell damage (PC) group ($P < 0.05$).

3.8. *In vitro antibacterial test*

In Fig. 6C, the viabilities of *S. epidermidis* in suspensions after 24 h of different treatments were presented by fluorescence images. The negative control (NC), FV-60A and PUA-BLK IOL groups showed numerous green spots (viable cells) in the field, whereas red spots (dead cells) but no green spots were observed in the groups treated with 2 μg/mL GAT

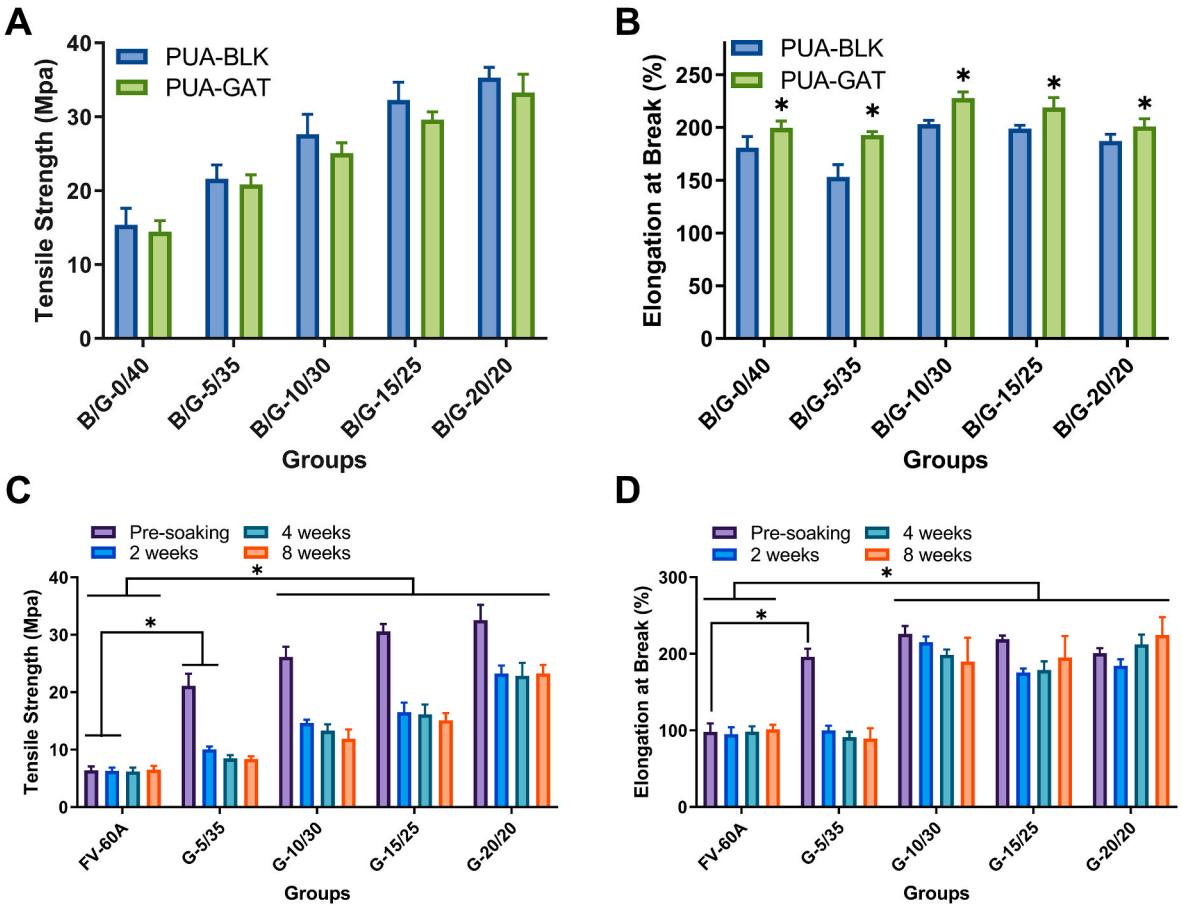

Fig. 5. The ultimate tensile strength (A) and the elongation (B) of PUA-BLK and PUA-GAT at dehydrated state (*: $P < 0.05$, multiple t tests); the variation of ultimate tensile strength (C) and elongation at break (D) of PUA-GAT and FV-60A with different hydration time in PBS (*: $P < 0.05$, two-way ANOVA with Sidak's multiple comparisons test).

solution and PUA-GAT IOL. This result indicated that the GAT released from the PUA-GAT IOL within the first 24 h has effectively controlled the bacterial proliferation. Also, the result establishes the foundation for any further investigation on the antibacterial ability of PUA-GAT IOL *in vivo*.

3.9. In vivo biocompatibility study

All operations of lens phacoemulsification with IOL implantations went successfully. Similar to the implantation of hydrophobic acrylic IOLs, the novel IOLs were used at dry state, they were folded and injected into lens capsular bags via IOL injection system without any extra procedure.

Through slit lamp examination, groups I, II, and III were compared in terms of post-operative inflammatory condition and complications (Fig. 7A). All eyes were normal before operation, and no exudation, hyphema, or hypopyon was found post-operatively. However, all operated eyes showed a slight to medium degree of acute inflammation symptoms, including conjunctival injection, chemosis, corneal edema, aqueous flare, and presence of cells in aqueous humor one day after surgery; these inflammation symptoms gradually alleviated and vanished before day 29. No significant difference in each inflammatory sign score was found among the groups in all fixed time points ($P > 0.05$) (SI in Fig. S9). Complication such as synechia occasionally appeared in all three groups after surgeries, and it was assumed to be operation damage.

Pathological examination further revealed the compatibility of PUA-GAT and PUA-BLK IOLs. No abnormal morphological feature was observed in the ocular tissues, and no obvious abnormalities were seen in the histological structure of the cornea, iris, and retina (Fig. 7B). Corneal endothelial cell density was measured pre-operatively and on day 29 post-operation, as shown in Fig. 7C, no significant cell loss was found among the three groups ($P > 0.05$). Moreover, no significant IOP change on day 29 post-operation was found in each group (SI in Fig. S8). All of the *in vivo* studies above revealed the good compatibility of the PUA-GAT and PUA-BLK IOLs.

3.10. In vivo drug release study

GAT concentration in aqueous humor is a reliable basis to directly assess the release level of the target drug *in vivo*. As presented in Fig. 7D, GAT concentration in the PUA-GAT IOL group was higher than that in the GAT topical dosing group for the first 5 days. The GAT concentration in group III reached 4.93 μg/mL within 15 min after IOL implantation, and the highest concentration of 6.18 μg/mL was measured after 1 h of implantation. Thereafter, the GAT concentration gradually decreased, and 0.70 μg/mL GAT was measured on day 29 after operation.

3.11. In vivo antibacterial test

All eyes were normal pre-operatively, and all surgeries done for the antibacterial study went smoothly. A day after the operation, signs of acute inflammation similar to those observed during the biocompatibility study were found in all operated eyes, and slight hyphema due to surgical injury was found in some of the eyes; however, no significant difference was observed among the groups before the endophthalmitis model was established by using *S. epidermidis*. As shown in Fig. 8A, all operated eyes in group B developed intraocular infection on day 2 post-

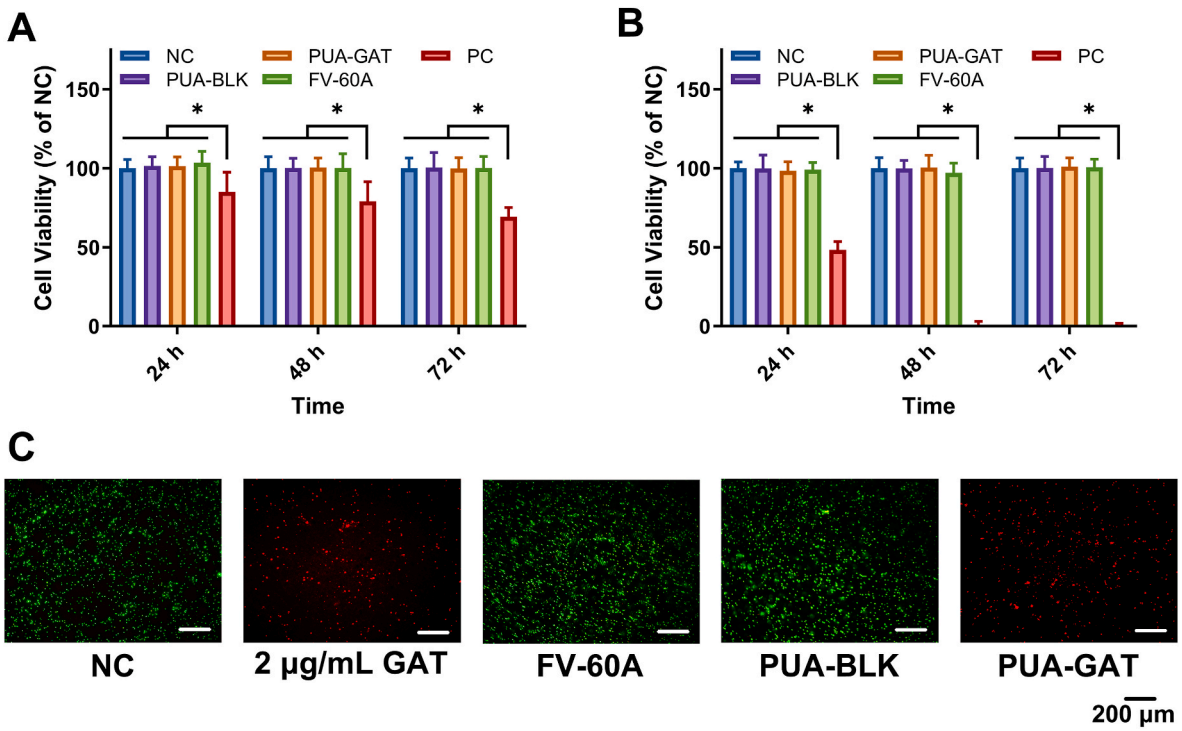

Fig. 6. CCK8 tests of cell viability of APRE-19 (A) and hLECs (B) after treating with normal medium (NC), PUA-BLK IOL, PUA-GAT IOL, FV-60A extractions and 5% DMSO contained medium (PC) for 24, 48 and 72 h (*: $P < 0.05$, two-way ANOVA with Sidak's multiple comparisons test); (C) Left to right: viability of fluorescent stained *S. epidermidis* of negative control (NC), FV-60A IOL, positive control (2 μg/mL GAT solution), PUA-BLK IOL and PUA-GAT IOL groups (green spots: live cells, red spots: dead cells), scale bar: 200 μm.

operation; this condition was characterized by apparent corneal opacity, hypopyon, exudation, severe aqueous flare, and a large amount of aqueous humor cells, and the conditions of ciliary injection, conjunctival injection, and edema were aggravated than the day before. By contrast, no signature of bacterial infection, such as hypopyon, was found in group C or group A. Severe aqueous flares were found in groups B and C on day 2; the other signs in group C were at the same level as in group A (Fig. 8B). Notably, fibrinous exudation, a symptom of acute inflammation caused by the sudden inrush of bacterial solution, was found in the anterior chamber in group C. All acute inflammatory conditions in groups A and C continued to improve. On day 15, the fibrinous exudation in group C was basically absorbed, but hypopyon was still observed in group B. On day 29 post-operation, the eyes in groups A and C had recovered from inflammation, and the posterior synechia had considerably improved. Conjunctival injection, corneal neovascularization, yellow cloudy fundus, and severe synechia were still presented in group B by the end of the study.

A further test indicated that the exudation in group C was aseptic. The aqueous humor collected from group C was transparent, whereas that collected from group B was turbid. After culture for 24 h, a number of white bacterial colonies were found in group B, whereas no colony was noticed in group C (Fig. 8C). The colony in group B was identified, and it matched the *S. epidermidis* strain that was used for the model. As regards the IOP of all the operated eyes (Fig. 8D), the average IOP in group B by the end of the study was significantly lower than that pre-operatively ($P < 0.05$). No abnormal change in IOP was found in groups A and C.

In group B, ocular atrophy of the operated eyes was presented on day 29. The equatorial diameter and the anteroposterior diameter of the operated eyes in group B were 16–17 and 15–16 mm, respectively; the contralateral eyes and eyes in group A and C measured 19–21 and 18–20 mm, respectively. Histological examination results were shown in Fig. 8E. Signs of endophthalmitis, including edema at corneal stroma, disarrangement of corneal endothelium structure, enlargement of iris vessels and disordered structure of iris, and tissue organization which was adhered to the retinal pigment epithelium with inflammatory infiltration, were observed in the tissue sections obtained from group B. In group C, no evidence of infection was observed at the pathological level; moreover, the intact and regular structure of cornea, iris, and fundus in group C were all similar to those in blank control group (group A), demonstrating the successful prevention of POE using PUA-GAT IOL.

4. Discussion

While multiple methods are applied to modify an IOL into a drug delivery device for preventing complications after cataract surgery, there is still space to seek a more advanced drug loading method. In this work, the possibility of developing a sustained GAT released foldable IOL based on PUA was investigated. The mild environment during polymerization, the rapid and extremely simplified process of fabrication, along with the exclusion of toxic reagent solvent offered by the means of bulk photocuring and DLP technology, has led to the secured stability of GAT, high drug uptake ability, in addition to good biocompatibility. The proposed GAT-loaded IOL also displayed controllable drug release behavior, easy implantation procedure, good optical properties, and moderate mechanical properties. The sustained GAT released IOL effectively prevented the occurrence of POE *in vivo*, making this novel IOL a promising ophthalmic anti-infection drug delivery device.

The drug loading capacity, effective release time, and drug concentration *in vivo*, which directly relates to the therapeutic effect, is important for a sustained drug release IOL. For an antibiotic that works in ocular tissues, an insufficient antibiotic concentration and short effective time result in unsatisfactory activity, whereas a high concentration may lead to intraocular toxicity. Therefore, when sufficient antibiotic supply is desired to get a satisfactory therapeutic effect toward POE, the release rate also needs to be controlled. However, the data of loading dose and release behavior about GAT-loaded IOLs in reported

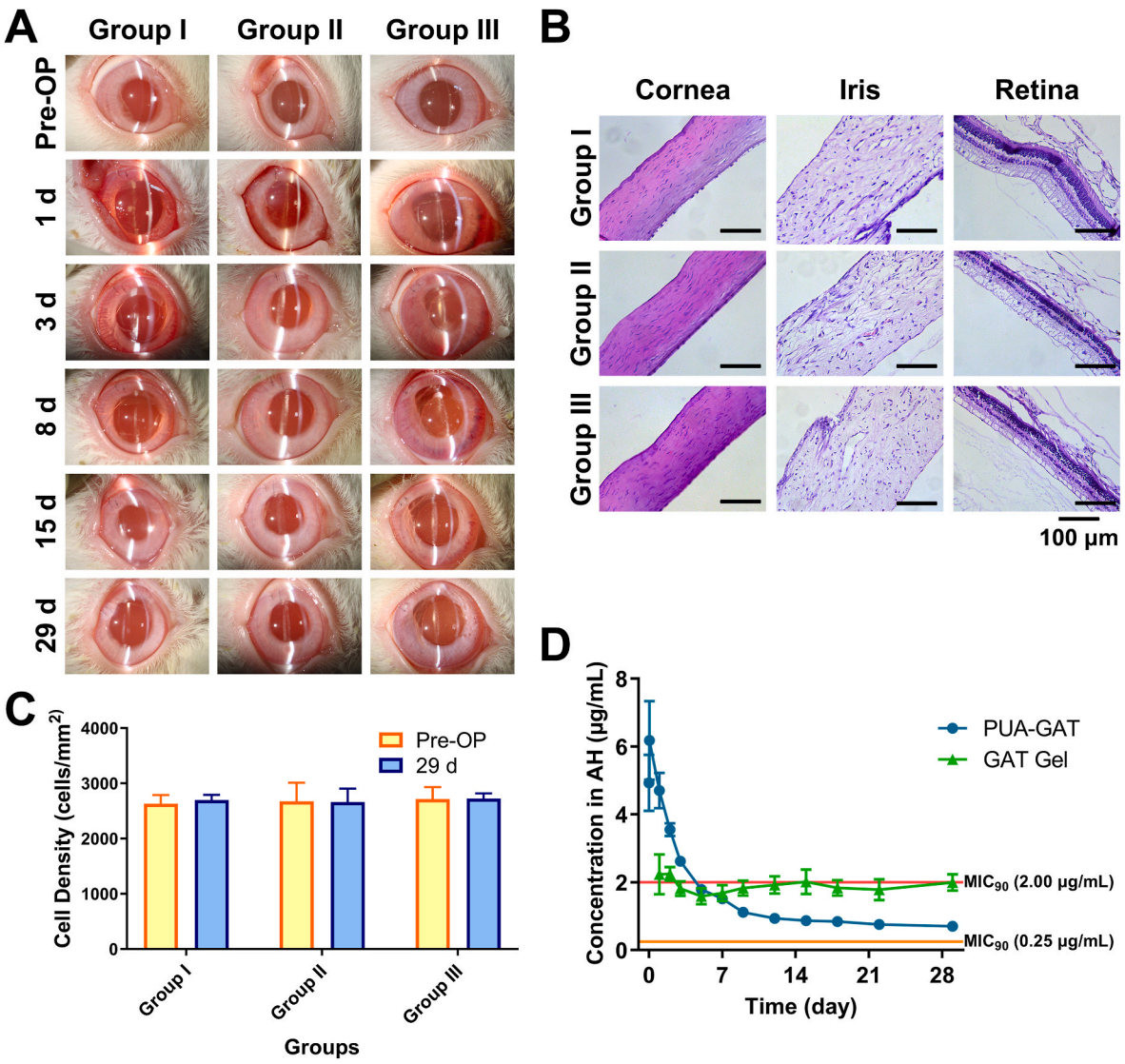

Fig. 7. *In vivo* biocompatibility evaluations with implantation of FV-60A IOL (Group I), PUA-BLK IOL (Group II) and PUA-GAT IOL (Group III): (A) Slit-lamp examination of anterior segment at different time points, slight inflammation including conjunctival injection, chemosis, corneal edema, aqueous flare, and presence of cells in aqueous humor was demonstrated in all group at the early stage after surgery, no severe inflammation was seen postoperatively; (B) Histological images of cornea, iris and retina on day 29 after implantation, regular and intact structures were found in all groups and no sign of severe inflammation was noticed, scale bar: 100 μm; (C) Corneal endothelial cell density pre-operation and on day 29 after implantation ($P > 0.05$, multiple t tests); (D) GAT concentration from PUA-GAT IOL and from topical GAT gel in aqueous humor (AH), wherein the horizon lines (in red and orange) represent two MIC_{90} of GAT towards *S. epidermidis* according to references.

approaches was improvable. The optimized impregnation yield of GAT in IOL via CO_2 supercritical impregnation process was 1.03 ± 0.07 μg/mg, only 24.0 ± 1.2 μg GAT was released in several weeks [56]. As reported of the solution presoaking method, though more than 70 μg GAT was released in the first 24 h, only 1.9 ± 0.8 μg/mL of GAT in aqueous humors was measured 2 h after *in vivo* implantation, which did not reach the MIC_{90} of *S. epidermidis* [27]. In the current study, an improved drug loading dose and release behavior, wherein it balanced the concentration and the release speed, was demonstrated. 5.10 ± 0.14 μg/mg of GAT in optimized group was released within 40 days. The GAT concentration in aqueous humor remained above the MIC_{90} of *S. epidermidis* for 5 days, which offered enough time to control the acute POE. GAT ophthalmic gel exhibited the best bioavailability in human aqueous humor compared to other common antibiotic ophthalmic solutions [57], however, the concentration of GAT decreased fast in ocular, and the effectiveness of topical administration always has been highly related to patient compliance and single dosage. Comparing to commercial GAT gel, GAT-loaded IOL exhibited higher GAT concentration in aqueous humor for days, which was crucial to prevent POE. It suggested that our IOL would provide a better prevention towards POE in the early post-operative period. In addition, the efficacy of GAT-loaded IOL will not be affected by external factors.

Driven by drug diffusion and polymer chain relaxation [58], the drug release process of non-degradable polymeric matrix–drug mixing system is influenced by complex factors, including the characteristics of the material matrix, wherein composition, structure and swelling were participated [59]. In this study, the management of the drug delivery behavior of GAT-loaded IOLs was completed by the alteration of the ingredients' proportion. The change of the ratio of hydrophilic bond and hydrophobic bond, offered by NVP and IBOMA respectively, resulted in a variety of polymeric matrixes with different chemical structure. The result that the drug release facilitated by a better surface hydrophilicity and higher swelling capacity in this study, was consistent with the swelling control theory [60–62]. Additionally, the bulky structure of

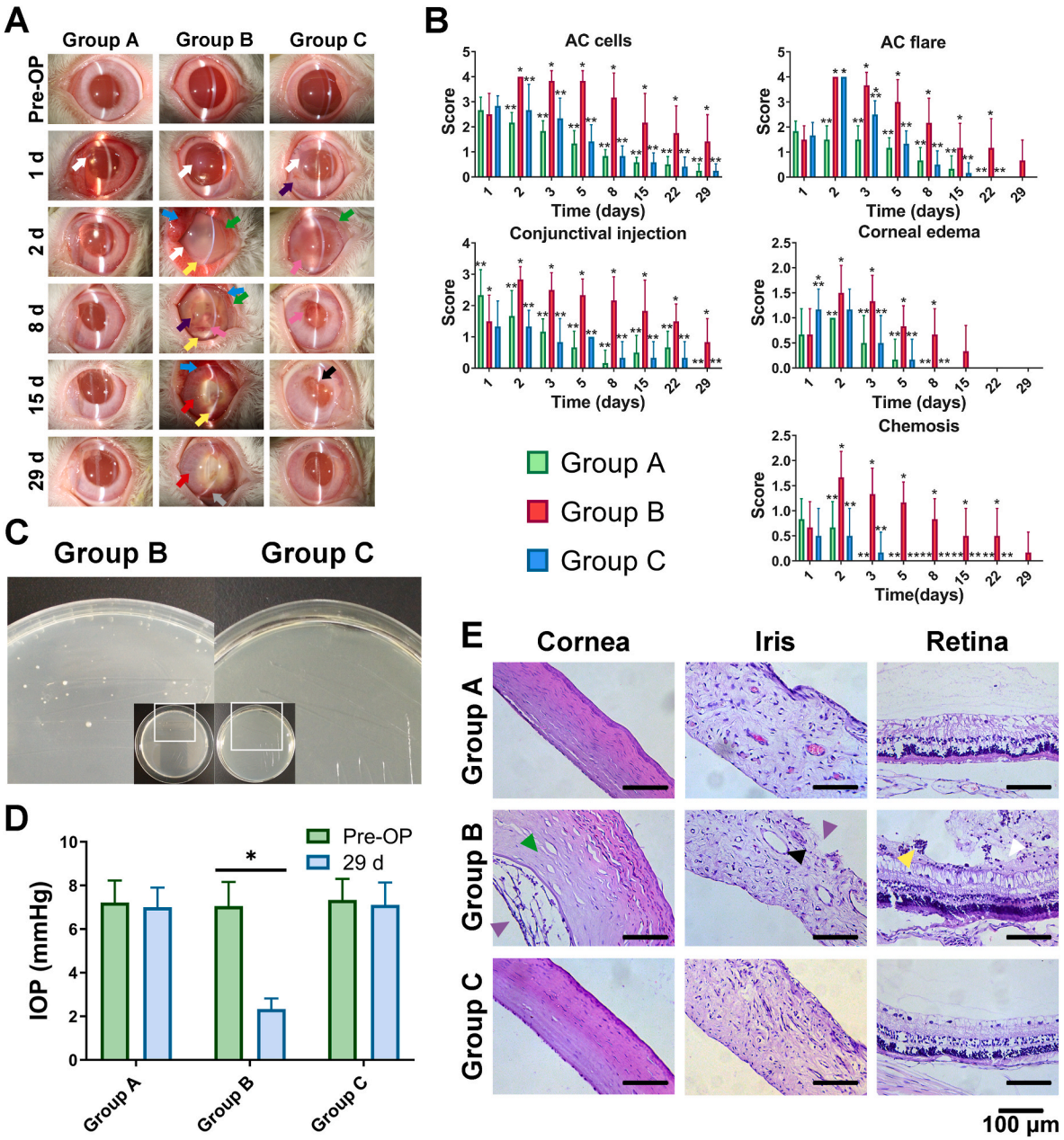

Fig. 8. *In vivo* antibacterial assessment of control group (Group A), infectious group (Group B) and PUA-GAT IOL group (Group C): (A) Slit-lamp examination of anterior segment at different time points (white arrow: cornea edema; purple arrow: blood exudation; blue arrow: conjunctival injection; green arrow: conjunctival edema; yellow arrow: hypopyon; pink arrow: exudation; red arrow: iris injection; black arrow: synechia; grey arrow: neovascular); (B) Grading of Anterior chamber (AC) cells, AC flares, conjunctival injection, corneal edema and chemosis after establishment of infectious postoperative endophthalmitis model (*: $P < 0.05$ when comparing to Group A at the same time point; **: $P < 0.05$ when comparing to Group B at the same time point; two-way ANOVA with Sidak's multiple comparisons test); (C) Aqueous humor culture of group B and group C, white spots: bacterial colonies; (D) Intraocular pressure pre-operation and on day 29 after implantation; (E) Histological images of cornea, iris and retina (green triangle: stroma edema; purple triangle: disordered structure; black triangle: enlarged vessel; yellow triangle: inflammatory cells; white triangle: organization and adherence of organization tissue with inflammatory cells), scale bar: 100 μm.

side chain of IBOMA could restrained the release rate by obstructing the diffusion path, according to the steric hindrance effect. Previous methods on controlling the drug release behavior of drug loaded IOLs always avoided changing the characteristics of the base matrix, mainly because of the inherent physical characteristics of the carrier IOLs were changeless. For those drugs which deposited in the polymeric matrix of IOLs, by solution soak or by supercritical fluid impregnation for instance, their release control depended on the change of the initial drug loading amount [27,63], however restricted control over the initial amount was presented. Our approach proved that the delivery behavior of drug-loaded IOLs could be adjusted by altering the characteristics of carrier IOL; this method has the complete control over the ingredients' programming and the initial drug amount, making the desirable release rate possible.

Besides the drug delivery performance, selected formula of PUA and co-reactants (IBOMA and NVP) brought GAT-loaded IOL long-term preservation, outstanding optical properties, proper mechanical properties, along with good biocompatibility. Exhibited data of surface contact angle and MC of acrylic IOLs [64–67] suggested this novel IOL belongs to the hydrophilic kind. A drawback about drug-eluting hydrophilic acrylates (hydrogels) IOL was that the constantly diffusion of drug into soaking solution during storage reduced the drug amount [68].

However, the low T_g of our copolymer, contributed by the soft segment of PUA, rendered it with foldable behavior under dehydrated state at room temperature, which was different from the rigid and fragile status of hydrogels that owned high T_g [69]. This distinctive feature enables the GAT-loaded IOL to be stored in dehydrated condition for long, it avoids the wastage of drug before unsealing. It follows the same implantation procedure of hydrophobic IOLs, it doesn't need pre-soaking or other treatments. Good optical properties are essential for a candidate IOL given that it works as an optical component in the visual pathway. IOLs made from pure PUR showed light transmittance less than 90% in visible wavelength range [41]. The participation of co-reactants in this current study has helped to increase the light transmittance by creating low crystalline structure and providing an entirely soluble environment for GAT and solid additives. As a result, the high light transmittance of PUA-GAT in the visible spectrum was comparable with commercial acrylates IOLs [70]. The purposed material also showed a moderate refractive index compared with commercial IOLs [41], and this result was considered ideal given that post-operative glare was reported to be positively correlated with the refractive index of IOL [71], whereas a low refractive index could negatively affect the IOL's thickness. In addition, blocking of UV light is attributed to RUVA-93, which is beneficial in preventing macular disorders, and IPDI made the aliphatic polyurethanes a better yellowing-resistant material since quinonization was avoided [72]. PUA-GAT also succeed in possessing a proper ductility and strength, which are key mechanical character for an IOL material. The proposed material showed a better performance in terms of these two indicators compared with the FV-60A material in work condition. These properties determine whether an IOL will remain intact when folding and unfolding; also, they indicate the stability of an IOL when being implanted or when an external shock occurs. The combination of IBOMA's rigid ring structure and high T_g [73,74] and the degree of polymer conversion effected by NVP [75] resulted in the mechanical changes when the IBOMA/NVP ratio varies.

After the evaluation of its drug release performance, optical properties, mechanical properties and biocompatibility, the new IOL is considered to be an efficient, transparent, ductile, and safe drug delivery device suitable for preventing POE effectively. Based on our efficient, economical, and environment-friendly means, researches on diversity fields can be inspired. Firstly, the prevention and treatment of more intraocular diseases can possibly be achieved by changing the target drug and by programming suitable formula using our method. Secondly, IOLs with different shapes can be easily obtained by adjusting the 3D prototyping model, so studies about simulating and optimizing the drug release behavior on various types of IOLs will be convenient. In addition, the drug-mixed photosensitive resin can work as a 3D printing ink and thus can be used in 3D bioprinting studies. Furthermore, this fast fabricate method can offer help for the individualized therapy in clinical work. However, there is still room for improvement of this present study. Shrinkage of copolymer was presented during photopolymerization due to the conversion of monomer to polymer, and extra resin was applied to cover the shrinkage. It aroused concerns about the negative effects of interface between the two layers. Although interface between homogeneous substance has little impact on light transmission because the layers share the same refractive index, and mechanical defect like tear or rupture of the sample was never appeared during the years of research, a more advanced way is desired to allay the concerns in the future. The evaluation of ageing resistance performance and the accurate regulation of IOL's diopter through a precise mold control were not covered in this study and are yet to be investigated in future studies.

5. Conclusion

In this work, a GAT-loaded IOL, designed as a sustained drug delivery device for preventing POE, was prepared based on PUA via photopolymerization with the aid of a customized 3D-printed mold. The GAT release profile demonstrated satisfying drug stability, release amount, and rate. The alteration of ingredients' proportions allowed the control of drug release behavior. The optical test results showed that the design demonstrated a high light transmittance, a UV blocking ability, and a moderate refractive index. Moreover, the mechanical test results proved that the GAT-loaded material enhanced the strain stress and elongation performances compared to the reference commercial acrylic IOL material, and our IOL was foldable in a dehydrated state at room temperature. Good biocompatibility and the successful prevention of infectious POE caused by *S. epidermidis* were confirmed both *in vitro* and *in vivo*. For the first time, we explored the feasibility of incorporating the target drug into polymer system before polymerization in the field of IOL, and proved that by this means, the drug loading capacity and release performance were optimized compared with some previous methods. In addition, the copolymer based on PUA improved the key mechanical properties of IOL. Our study demonstrates that this GAT-loaded IOL is a qualified drug delivery implantation, and this approach provides the basis for various studies and potential applications in ophthalmology and other medical fields.

Ethics approval and consent to participate

We confirm that any aspect of the work covered in this manuscript that has involved experimental animals has been conducted with the ethical approval of all relevant bodies and that such approvals are acknowledged within the manuscript.

CRediT authorship contribution statement

Mengna Li: Conceptualization, Methodology, Investigation, Data curation, Formal analysis, Writing – original draft, Software, Visualization. **Jing-Wei Xu:** Conceptualization, Methodology, Investigation, Writing – review & editing. **Jiayong Li:** Investigation, Data curation, Formal analysis. **Wei Wang:** Investigation, Funding acquisition, Validation. **Chenqi Luo:** Resources, Project administration. **Haijie Han:** Writing – review & editing. **Zhi-Kang Xu:** Conceptualization, Writing – review & editing, Supervision. **Ke Yao:** Funding acquisition, Conceptualization, Methodology, Writing – review & editing, Supervision.

Declaration of competing interest

An application for patent for the preparing method for a drug-loaded IOL described herein has been licensed [CN patent no. 201910376178.9] and issued to Zhejiang University. Other than that, we confirm that there are no conflicts of interest associated with this publication and there has been no significant financial support for this work that could have influenced its outcome.

Acknowledgments

We are grateful for the support from the crew of MOE Key Laboratory of Macromolecular Synthesis and Functionalization of Zhejiang University, and thanks to Prof. Tao Xie and PhD. Limei Huang from State Key Laboratory of Chemical Engineering of Zhejiang University for the DLP printing technique support. Funding was provided by the Program of National Natural Science Foundation of China [81870641, 82070939] and Key Research and Development Program of Zhejiang Province of China [2020C03035].

Appendix A. Supplementary data

Supplementary data to this article can be found online at https://doi.org/10.1016/j.bioactmat.2022.05.032.

References

[1] D. Pascolini, S.P. Mariotti, Global estimates of visual impairment: 2010, Br. J. Ophthalmol. 96 (2012) 614–618, https://doi.org/10.1136/bjophthalmol-2011-300539.

[2] Y. Liu, M. Wilkins, T. Kim, B. Malyugin, J.S. Mehta, Cataracts, Lancet 390 (2017) 600–612, https://doi.org/10.1016/S0140-6736(17)30544-5.

[3] H. Verbraeken, Treatment of postoperative endophthalmitis, Ophthalmologica 209 (1995) 165–171, https://doi.org/10.1159/000310605.

[4] H. Cao, L. Zhang, L. Li, S. Lo, Risk factors for acute endophthalmitis following cataract surgery: a systematic review and meta-analysis, PLoS One 8 (2013), e71731, https://doi.org/10.1371/journal.pone.0071731.

[5] M. Moshirfar, V. Feiz, A.T. Vitale, J.A. Wegelin, S. Basavanthappa, D.H. Wolsey, Endophthalmitis after uncomplicated cataract surgery with the use of fourth-generation fluoroquinolones: a retrospective observational case series, Ophthalmology 114 (2007) 686–691, https://doi.org/10.1016/j.ophtha.2006.08.038.

[6] E.E. Freeman, M.-H. Roy-Gagnon, E. Fortin, D. Gauthier, M. Popescu, H. Boisjoly, Rate of endophthalmitis after cataract surgery in Quebec, Canada, 1996-2005, Arch. Ophthalmol. 128 (2010) 230–234, https://doi.org/10.1001/archophthalmol.2009.380.

[7] R.C. Khanna, C. Garudadri, Incidence of post-cataract endophthalmitis at aravind eye hospital, Indian J. Ophthalmol. 58 (2010), https://doi.org/10.4103/0301-4738.71704, 562-562.

[8] C.C. Wykoff, M.B. Parrott, H.W. Flynn Jr., W. Shi, D. Miller, E.C. Alfonso, Nosocomial acute-onset postoperative endophthalmitis at a university teaching hospital (2002-2009), Am. J. Ophthalmol. 150 (2010) 392–398, https://doi.org/10.1016/j.ajo.2010.04.010, e2.

[9] K. Yao, Y. Zhu, Z. Zhu, J. Wu, Y. Liu, Y. Lu, Y. Hao, Y. Bao, J. Ye, Y. Huang, Z. Li, X. Shentu, Y. Yu, The incidence of postoperative endophthalmitis after cataract surgery in China: a multicenter investigation of 2006–2011, Br. J. Ophthalmol. 97 (2013) 1312, https://doi.org/10.1136/bjophthalmol-2013-303282.

[10] European Society of Cataract and Refractive Surgeons, ESCRS Guidelines for Prevention and Treatment of Endophthalmitis Following Cataract Surgery: Data, Dilemmas and Conclusions, https://www.escrs.org/endophthalmitis/guidelines/ENGLISH_2018_updated.pdf. (Accessed Apr 1 2022).

[11] H. Liu, L. Wu, S. Fu, Y. Hou, P. Liu, H. Cui, J. Liu, L. Xing, X. Zhang, Polylactide-glycoli acid and rapamycin coating intraocular lens prevent posterior capsular opacification in rabbit eyes, Graef. Arch. Clin. Exp. 247 (2009) 801–807, https://doi.org/10.1007/s00417-008-1007-0.

[12] M.C. Boffa, D. Labarre, M. Jozefowicz, G.A. Boffa, Interactions between human plasma proteins and heparin-poly(methyl methacrylate) copolymer, Thromb. Haemostasis 41 (1979) 346–356.

[13] X. Zhang, K. Lai, S. Li, J. Wang, J. Li, W. Wang, S. Ni, B. Lu, A. Grzybowski, J. Ji, H. Han, K. Yao, Drug-eluting intraocular lens with sustained bromfenac release for conquering posterior capsular opacification, Bioact. Mater. 9 (2022) 343–357, https://doi.org/10.1016/j.bioactmat.2021.07.015.

[14] J. Qie, S. Wen, Y. Han, S. Liu, L. Shen, H. Chen, Q. Lin, A polydopamine-based photodynamic coating on the intraocular lens surface for safer posterior capsule opacification conquering, Biomater. Sci. 10 (2022) 2188–2197, https://doi.org/10.1039/D2BM00038E.

[15] D. Lu, Y. Han, D. Liu, S. Chen, J. Qie, J. Qu, Q. Lin, Centrifugally concentric ring-patterned drug-loaded polymeric coating as an intraocular lens surface modification for efficient prevention of posterior capsular opacification, Acta Biomater. 138 (2022) 327–341, https://doi.org/10.1016/j.actbio.2021.11.018.

[16] H. Huang, S. Zhu, Y. Han, D. Liu, S. Liu, D. Lu, R. Wang, Q. Lin, Cascade catalytic platform modified intraocular lens for high-efficient posterior capsule opacification prevention, Chem. Eng. J. 427 (2022), https://doi.org/10.1016/j.cej.2021.131553, 131553.

[17] S. Liu, X. Zhao, J. Tang, Y. Han, Q. Lin, Drug-eluting hydrophilic coating modification of intraocular lens via facile dopamine self-polymerization for posterior capsular opacification prevention, ACS Biomater. Sci. Eng. 7 (2021) 1065–1073, https://doi.org/10.1021/acsbiomaterials.0c01705.

[18] L. Lin, Y. Wang, X. Huang, Z. Xu, K. Yao, Modification of hydrophobic acrylic intraocular lens with poly(ethylene glycol) by atmospheric pressure glow discharge: a facile approach, Appl. Surf. Sci. 256 (2010) 7354–7364, https://doi.org/10.1016/j.apsusc.2010.05.068.

[19] J. Xia, D. Lu, Y. Han, J. Wang, Y. Hong, P. Zhao, Q. Fang, Q. Lin, Facile multifunctional IOL surface modification via poly(PEGMA-co-GMA) grafting for posterior capsular opacification inhibition, RSC Adv. 11 (2021) 9840–9848, https://doi.org/10.1039/D1RA00201E.

[20] J. Xia, Y. Han, L. Shen, R. Wang, S. Wen, S. Zhu, Q. Lin, Photo-responsive intraocular lens with on demand drug release for posterior capsule opacification prevention and improved biosafety, Chem. Eng. J. 430 (2022), https://doi.org/10.1016/j.cej.2021.132716, 132716.

[21] S. Zhu, H. Huang, D. Liu, S. Wen, L. Shen, Q. Lin, Augmented cellular uptake and homologous targeting of exosome-based drug loaded IOL for posterior capsular opacification prevention and biosafety improvement, Bioact. Mater. 15 (2022) 469–481, https://doi.org/10.1016/j.bioactmat.2022.02.019.

[22] M. Saraswathy, K. Sreenivasan, Layer-by-Layer modification of Poly (methyl methacrylate) intra ocular lens: drug delivery applications, Pharmaceut. Dev. Technol. 15 (2009) 379–385, https://doi.org/10.3109/10837450903262025.

[23] C. Qin, S. Liu, S. Wen, Y. Han, S. Chen, J. Qie, H. Chen, Q. Lin, Enhanced PCO prevention of drug eluting IOLs via endocytosis and autophagy effects of a PAMAM dendrimer, J. Mater. Chem. B. 9 (2021) 793–800, https://doi.org/10.1039/D0TB02530E.

[24] S. Eperon, M. Rodriguez-Aller, K. Balaskas, R. Gurny, Y. Guex-Crosier, A new drug delivery system inhibits uveitis in an animal model after cataract surgery, Int. J. Pharm. 443 (2013) 254–261, https://doi.org/10.1016/j.ijpharm.2012.12.033.

[25] S. Garty, R. Shirakawa, A. Warsen, E.M. Anderson, M.L. Noble, J.D. Bryers, B. D. Ratner, T.T. Shen, Sustained antibiotic release from an intraocular lens–hydrogel assembly for cataract surgery, Invest. Ophthalmol. Vis. Sci. 52 (2011) 6109–6116, https://doi.org/10.1167/iovs.10-6071.

[26] H. Matsushima, K. Mukai, N. Gotoo, S. Yoshida, T. Yoshida, M. Sawano, T. Senoo, Y. Obara, J.I. Clark, The effects of drug delivery via hydrophilic acrylic (hydrogel) intraocular lens systems on the epithelial cells in culture, Ophthalmic Surg. Laser. Imag. 36 (2005) 386–392, https://doi.org/10.3928/1542-8877-20050901-07.

[27] I. Lipnitzki, R. Bronshtein, S. Ben Eliahu, A.L. Marcovich, G. Kleinmann, Hydrophilic acrylic intraocular lens as a drug delivery system: influence of the presoaking time and comparison to intracameral injection, J. Ocul. Pharmacol. Therapeut. 29 (2013) 414–418, https://doi.org/10.1089/jop.2012.0062.

[28] C. González-Chomón, M.E.M. Braga, H.C. de Sousa, A. Concheiro, C. Alvarez-Lorenzo, Antifouling foldable acrylic IOLs loaded with norfloxacin by aqueous soaking and by supercritical carbon dioxide technology, Eur. J. Pharm. Biopharm. 82 (2012) 383–391, https://doi.org/10.1016/j.ejpb.2012.07.007.

[29] A. Bouledjouidja, Y. Masmoudi, Y. Li, W. He, E. Badens, Supercritical impregnation and optical characterization of loaded foldable intraocular lenses using supercritical fluids, J. Cataract Refract. Surg. 43 (2017) 1343–1349, https://doi.org/10.1016/j.jcrs.2017.07.033.

[30] U.S. National Library of Medicine, Modified Intraocular Lens to Reduce Eye Inflammation after Cataract Surgery in Uveitis Patients, 2002. https://www.clinicaltrials.gov/ct2/show/NCT00001311. (Accessed 1 April 2022). Accessed.

[31] U.S. National Library of Medicine, Safety and Efficacy of a Heparin-Coated Intraocular Lens in Uveitis, 1999. https://clinicaltrials.gov/ct2/show/NCT00000119. (Accessed 1 April 2022). Accessed.

[32] U.S. National Library of Medicine, Aqueous Flare of a Hydrophobic Acrylic Single-Piece Open-Loop IOL with Modified Material Surface Properties, 2013. https://clinicaltrials.gov/ct2/show/NCT01767012. (Accessed 1 April 2022). Accessed.

[33] R.A. Scott, N.A. Peppas, Highly crosslinked, PEG-containing copolymers for sustained solute delivery, Biomaterials 20 (1999) 1371–1380, https://doi.org/10.1016/S0142-9612(99)00040-X.

[34] J.H. Ward, N.A. Peppas, Preparation of controlled release systems by free-radical UV polymerizations in the presence of a drug, J. Contr. Release 71 (2001) 183–192, https://doi.org/10.1016/S0168-3659(01)00213-9.

[35] G. Debellemanière, M. Flores, M. Montard, B. Delbosc, M. Saleh, Three-dimensional printing of optical lenses and ophthalmic surgery: challenges and perspectives, J. Refract. Surg. 32 (2016) 201–204, https://doi.org/10.3928/1081597X-20160121-05.

[36] G. Taormina, C. Sciancalepore, M. Messori, F. Bondioli, 3D printing processes for photocurable polymeric materials: technologies, materials, and future trends, J. Appl. Biomater. Funct. Mater. 16 (2018) 151–160, https://doi.org/10.1177/2280800018764770.

[37] M.J. Kang, C.K. Joo, Three cases of a torn haptic after scleral fixation using a hydrophobic acrylic intraocular lens: case reports, Medicine 97 (2018), https://doi.org/10.1097/MD.0000000000009853 e9853.

[38] K. Örnek, A. Ergin, T. Oğurel, Fracture of hydrophilic acrylic intraocular lens during cataract surgery, J. Cataract Refract. Surg. 34 (2008) 525, https://doi.org/10.1016/j.jcrs.2007.11.017.

[39] J.Y. Lee, J.Y. Kim, Optic fracture of the preloaded intraocular lens during insertion, Kor. J. Ophthalmol. 30 (2016) 79–80, https://doi.org/10.3341/kjo.2016.30.1.79.

[40] P. Bruin, E.A. Meeuwsen, M.V. van Andel, J.G. Worst, A.J. Pennings, Autoclavable highly cross-linked polyurethane networks in ophthalmology, Biomaterials 14 (1993) 1089–1097, https://doi.org/10.1016/0142-9612(93)90210-s.

[41] D. Bozukova, V. Bertrand, C. Pagnoulle, M.-C. De Pauw-Gillet, Evaluation of a class of polyurethane materials for intraocular lens manufacturing, J. Biomed. Mater. Res. B Appl. Biomater. 103 (2015) 1274–1286, https://doi.org/10.1002/jbm.b.33305.

[42] J.H. de Groot, C.J. Spaans, R.V. van Calck, F.J. van Beijma, S. Norrby, A. J. Pennings, Hydrogels for an accommodating intraocular lens, An explorative study, Biomacromolecules. 4 (2003) 608–616, https://doi.org/10.1021/bm0257053.

[43] W.L. Jongebloed, G. van der Veen, D. Kalicharan, M.V. van Andel, G. Bartman, J.G. F. Worst, New material for low-cost intraocular lenses, Biomaterials 15 (1994) 766–773, https://doi.org/10.1016/0142-9612(94)90030-2.

[44] S.D. Maurya, S.K. Kurmvanshi, S. Mohanty, S.K. Nayak, A review on acrylate-terminated urethane oligomers and polymers: synthesis and applications, Polym. Plast. Technol. Eng. 57 (2018) 625–656, https://doi.org/10.1080/03602559.2017.1332764.

[45] C. Perry, D. Ormrod, M. Hurst, S. Onrust, Gatifloxacin: a review of its use in the management of bacterial infections, Drugs 62 (2002) 169–207, https://doi.org/10.2165/00003495-200262010-00007.

[46] L.P. Bellini, G.M. Martins, M.C. Bulla, Preventing endophthalmitis after cataract surgeries, Br. J. Ophthalmol. 95 (2011) 892–893, https://doi.org/10.1136/bjo.2011.205039.

[47] T. Wada, S. Kozai, T. Tajika, H. Sakaki, T. Suzuki, Y. Ohashi, Prophylactic efficacy of ophthalmic quinolones in experimental endophthalmitis in rabbits, J. Ocul. Pharmacol. Therapeut. 24 (2008) 278–289, https://doi.org/10.1089/jop.2007.0121.

[48] M.S. Benz, I.U. Scott, H.W. Flynn Jr., N. Unonius, D. Miller, Endophthalmitis isolates and antibiotic sensitivities: a 6-year review of culture-proven cases, Am. J. Ophthalmol. 137 (2004) 38–42, https://doi.org/10.1016/s0002-9394(03)00896-1.

[49] G. Torkildsen, J.W. Proksch, A. Shapiro, S.K. Lynch, T.L. Comstock, Concentrations of besifloxacin, gatifloxacin, and moxifloxacin in human conjunctiva after topical ocular administration, Clin. Ophthalmol. 4 (2010) 331–341, https://doi.org/10.2147/opth.s9163.
[50] M. Long, H.G. Jensen, A.G.S. Group, Ocular bacteria from conjunctivitis patients: susceptibility to gatifloxacin and older fluoroquinolones, Invest. Ophthalmol. Vis. Sci. 44 (2003) 2115.
[51] ISO, Plastics — Determination of Tensile Properties, Part 2: Test Conditions for Moulding and Extrusion Plastics, 2012, p. 11. Switzerland.
[52] S. Li, Z. Lu, Y. Huang, Y. Wang, Q. Jin, X. Shentu, J. Ye, J. Ji, K. Yao, H. Han, Anti-oxidative and anti-inflammatory micelles: break the dry eye vicious cycle, Adv. Sci. (2022), https://doi.org/10.1002/advs.202200435, 2200435.
[53] J.H. Draize, G. Woodard, H.O. Calvery, Methods for the study of irritation and toxicity of substances applied topically to the skin and mucous membranes, J. Pharmacol. Exp. Therapeut. 82 (1944) 377–390.
[54] W.A. Chambers, S. Green, K.C. Gupta, R.N. Hill, K. Huntley, P.M. Hurley, L. A. Lambert, C.C. Lee, J.K. Lee, P.T. Liu, Scoring for eye irritation tests, Food Chem. Toxicol. 31 (1993) 111–115, https://doi.org/10.1016/0278-6915(93)90123-g.
[55] D.A. Jabs, R.B. Nussenblatt, J.T. Rosenbaum, Standardization of uveitis nomenclature working group, standardization of uveitis nomenclature for reporting clinical data. Results of the first international workshop, Am. J. Ophthalmol. 140 (2005) 509–516, https://doi.org/10.1016/j.ajo.2005.03.057.
[56] K. Ongkasin, Y. Masmoudi, T. Tassaing, G. Le-Bourdon, E. Badens, Supercritical loading of gatifloxacin into hydrophobic foldable intraocular lenses – process control and optimization by following in situ CO2 sorption and polymer swelling, Int. J. Pharm. 581 (2020), https://doi.org/10.1016/j.ijpharm.2020.119247, 119247.
[57] W. Ding, W. Ni, H. Chen, J. Yuan, X. Huang, Z. Zhang, Y. Wang, Y. Yu, K. Yao, Comparison of drug concentrations in human aqueous humor after the administration of 0.3% gatifloxacin ophthalmic gel, 0.3% gatifloxacin and 0.5% levofloxacin ophthalmic solutions, Int. J. Med. Sci. 12 (2015) 517–523, https://doi.org/10.7150/ijms.11376.
[58] W.B. Liechty, D.R. Kryscio, B.V. Slaughter, N.A. Peppas, Polymers for drug delivery systems, Annu. Rev. Chem. Biomol. Eng. 1 (2010) 149–173, https://doi.org/10.1146/annurev-chembioeng-073009-100847.
[59] Y. Fu, W.J. Kao, Drug release kinetics and transport mechanisms of non-degradable and degradable polymeric delivery systems, Expert Opin, Drug Deliv. 7 (2010) 429–444, https://doi.org/10.1517/17425241003602259.
[60] M. Efentakis, M. Vlachou, N.H. Choulis, Effects of excipients on swelling and drug release from compressed matrices, Drug Dev. Ind. Pharm. 23 (1997) 107–112, https://doi.org/10.3109/03639049709148487.
[61] M. Danckwerts, A. Fassihi, Implantable controlled release drug delivery systems: a review, Drug Dev. Ind. Pharm. 17 (1991) 1465–1502, https://doi.org/10.3109/03639049109026629.
[62] N.A. Peppas, P. Bures, W. Leobandung, H. Ichikawa, Hydrogels in pharmaceutical formulations, Eur. J. Pharm. Biopharm. 50 (2000) 27–46, https://doi.org/10.1016/S0939-6411(00)00090-4.
[63] A. Bouledjouidja, Y. Masmoudi, M. Sergent, V. Trivedi, A. Meniai, E. Badens, Drug loading of foldable commercial intraocular lenses using supercritical impregnation, Int. J. Pharm. 500 (2016) 85–99, https://doi.org/10.1016/j.ijpharm.2016.01.016.
[64] C.M. Cunanan, M. Ghazizadeh, S.Y. Buchen, P.M. Knight, Contact-angle analysis of intraocular lenses, J. Cataract Refract. Surg. 24 (1998) 341–351, https://doi.org/10.1016/s0886-3350(98)80322-2.
[65] R. Bellucci, An introduction to intraocular lenses: material, optics, haptics, design and aberration, in: J.L. Güell (Ed.), Cataract. ESASO Course Series, Karger, Basel, 2013, pp. 38–55.
[66] M. Tetz, M.R. Jorgensen, New hydrophobic IOL materials and understanding the science of glistenings, Curr. Eye Res. 40 (2015) 969–981, https://doi.org/10.3109/02713683.2014.978476.
[67] N. Yang, D.-D. Zhang, X.-D. Li, Y.-Y. Lu, X.-H. Qiu, J.-S. Zhang, J. Kong, Topography, wettability, and electrostatic charge consist major surface properties of intraocular lenses, Curr. Eye Res. 42 (2017) 201–210, https://doi.org/10.3109/02713683.2016.1164187.
[68] C. González-Chomón, A. Concheiro, C. Alvarez-Lorenzo, Drug-eluting intraocular lenses, Materials 4 (2011) 1927–1940, https://doi.org/10.3390/ma4111927.
[69] M. Tehrani, H.B. Dick, B. Wolters, T. Pakula, E. Wolf, Material properties of various intraocular lenses in an experimental study, Ophthalmologica 218 (2004) 57–63, https://doi.org/10.1159/000074568.
[70] J.M. Artigas, A. Felipe, A. Navea, C. Artigas, M.C. García-Domene, Spectral transmittance of intraocular lenses under natural and artificial illumination: criteria analysis for choosing a suitable filter, Ophthalmology 118 (2011) 3–8, https://doi.org/10.1016/j.ophtha.2010.06.023.
[71] J.C. Erie, M.H. Bandhauer, J.W. McLaren, Analysis of postoperative glare and intraocular lens design, J. Cataract Refract. Surg. 27 (2001) 614–621, https://doi.org/10.1016/S0886-3350(00)00781-1.
[72] D.K. Lee, H.B. Tsai, Properties of segmented polyurethanes derived from different diisocyanates, J. Appl. Polym. Sci. 75 (2000) 167–174, https://doi.org/10.1002/(SICI)1097-4628(20000103)75:1<167::AID-APP19>3.0.CO;2-N.
[73] S. Cousinet, A. Ghadban, E. Fleury, F. Lortie, J.P. Pascault, D. Portinha, Toward replacement of styrene by bio-based methacrylates in unsaturated polyester resins, Eur. Polym. J. 67 (2015) 539–550, https://doi.org/10.1016/j.eurpolymj.2015.02.016.
[74] B. Steyrer, P. Neubauer, R. Liska, J. Stampfl, Visible light photoinitiator for 3D-printing of tough methacrylate resins, Materials 10 (2017) 1445, https://doi.org/10.3390/ma10121445.
[75] T.J. White, W.B. Liechty, C.A. Guymon, The influence of N-vinyl pyrrolidone on polymerization kinetics and thermo-mechanical properties of crosslinked acrylate polymers, J. Polym. Sci. A. Polym. Chem. 45 (2007) 4062–4073, https://doi.org/10.1002/pola.22173.